

## Nondestructive Elastic Property Characterization of IC Encapsulants

Sridhar Canumalla and Michael G. Oravecz

Sonoscan, Inc., 530 E. Green Street  
Bensenville Illinois 60106, USA.  
(630) 766-7088/4603 (fax)  
sonoscan@worldnet.att.net

### ABSTRACT

The elastic properties of IC packaging materials (molding compounds and underfills) are measured nondestructively, over a microscopic area, in this study. The first application involves determining the engineering moduli of molding compounds (MP8000CH, MP190ML, 6300HA and 7320) from a nondestructive measurement of ultrasonic velocities. The second application involves the characterization of processing flaws in flip-chip packages to a) unambiguously identify delaminations (or voids) from resin rich areas, and b) quantitatively estimate the relative change in filler content. Concomitant changes in elastic properties of the underfill are also determined. Regions of filler segregation, exhibiting a lower impedance of about 3.9 MRayl (26% lower) are estimated to have a Young's modulus of 7 GPa (50% lower) and a CTE of  $41 \times 10^{-6}/^{\circ}\text{C}$  (57% higher than the base material). Techniques presented in this paper have potential application in advanced process control, yield management and in analysis of package reliability.

### INTRODUCTION

Plastics used in electronic packaging are engineered to achieve specified mechanical properties by the addition of various additives such as fillers. Due to processing variations, these properties may vary sufficiently to affect the package reliability (Suryanarayana et al., 1991). Knowledge of the relative variation in these properties, as well as the absolute values, could help in advanced process control, rapid yield management, and package reliability studies (such as finite element analysis). The properties of interest, such as stiffness and strength, should preferably be measured on production packages, nondestructively and over a microscopic area. Ultrasound, and specifically acoustic microscopy, is investigated for making these measurements in this study.

The acoustic microscope has been widely used as a metrology tool for detecting and characterizing flaws in electronic packages (for example, Taylor et al., 1997). High frequency ultrasound propagates through the package as an elastic

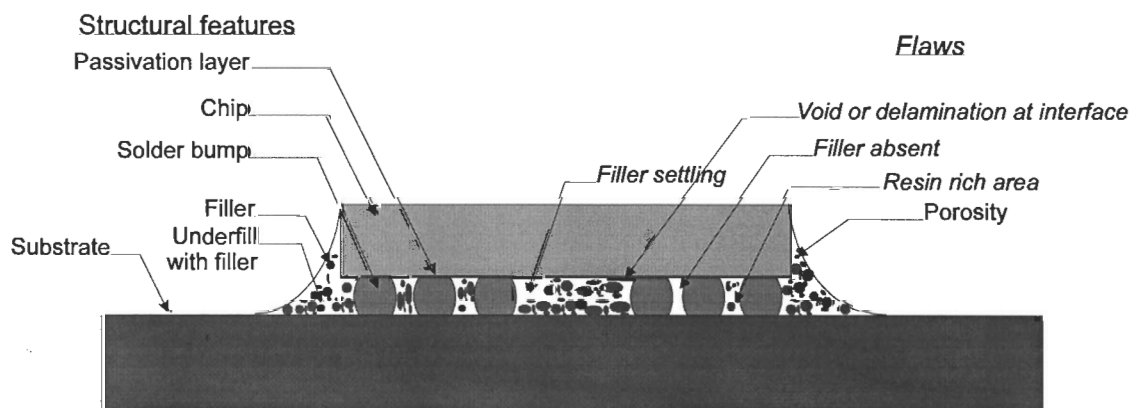
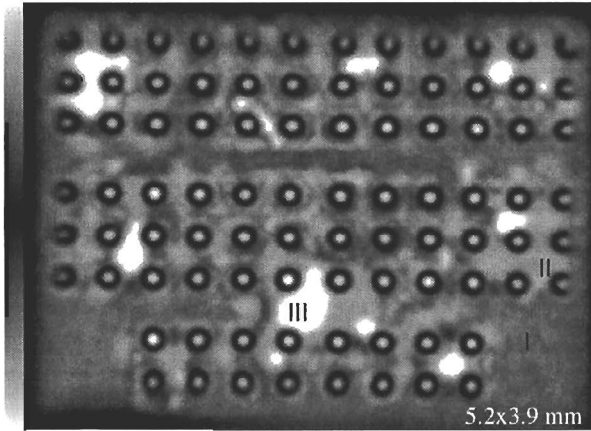


Figure 1. Schematic of a typical flip chip showing some processing flaws of interest.

disturbance, and the material properties modify the ultrasonic wave during propagation. This relationship has been widely utilized in characterizing the material properties nondestructively (for example, Canumalla et al., 1997). Results of an earlier investigation (Canumalla and Kessler, 1997) found ultrasonic velocity and attenuation varied significantly between molding compounds. This indicated that ultrasound could be sensitive to variations in composition in these molding compounds, and that ultrasonic parameters could be used to monitor changes in material parameters.



**Figure 2. Acoustic image of the die/underfill interface showing areas of different brightness I) normal background II) light gray areas III) bright white areas.**

The primary purpose of encapsulating flip-chips is to enhance the reliability of the package. Processing related inhomogeneities, such as filler segregation and voids, have been found to degrade fatigue life (Suryanarayana et al., 1991). Some typical flaws are shown schematically in Figure 1. Nondestructive inspections of flip-chip underfills, routinely achieved through

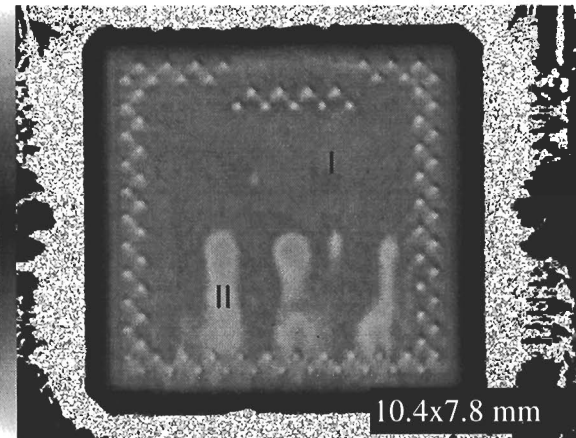


**Figure 3. Acoustic image of a flip chip sample revealing processing variations as areas of different brightness I) normal background II) lighter gray fingers.**

acoustic microscopy, can reveal inhomogeneities in the underfill, as illustrated in Figure 2 and 3, but the elastic properties of these inhomogeneities are not readily revealed. Information about the elastic properties, such as actual stiffness and CTE in these regions, could help in a more precise determination of their effect on reliability.

The goal of this study is to measure the engineering moduli of molding compounds used in IC package encapsulation and quantitatively characterize process variations observed in the underfill of flip-chip packages.

## THEORY

### Engineering Moduli of Molding Compounds with Ultrasound

In order to determine the engineering moduli via ultrasonic techniques, density ( $\rho$ ), shear velocity ( $V_s$ ), and compressional velocity ( $V_c$ ) need to be measured. The engineering moduli are calculated using Equations 1a to d:

$$\left. \begin{aligned} \text{Shear Modulus } \mu &= \rho V_s^2 \\ \text{Bulk Modulus } \kappa &= \rho \left( V_c^2 - 4 \frac{V_s^2}{3} \right) \\ \text{Young's Modulus } E &= \frac{\rho V_s^2 (3V_c^2 - 4V_s^2)}{V_c^2 - V_s^2} \\ \text{Poisson's Ratio } \nu &= \frac{E}{2\mu} - 1 \end{aligned} \right\} \quad (1 \text{ a-d})$$

The velocities are calculated using:

$$V_s = 2d / \Delta t_s \quad \text{and} \quad V_c = 2d / \Delta t_c \quad (2)$$

The procedure for measuring the compressional ( $\Delta t_c$ ) and shear wave ( $\Delta t_s$ ) time of flights is discussed in the Experiment section. In this work, the thickness was measured with a micrometer, and the mass density was taken from the manufacturers' data sheets.

Another ultrasonic parameter used to describe the reflection and transmission of ultrasound at interfaces between two materials is the acoustic impedance, which is defined as:

$$Z_c = \rho V_c \quad (3)$$

The compressional wave acoustic impedance, defined here, is the most commonly used, and will be used later in characterizing the processing variations in underfills.

In a previous study (Canumalla and Kessler, 1997), the acoustic impedances of molding compounds were measured using acoustic microscopy. Those values are used for a comparison of the theoretical acoustic impedance values calculated in this study (using the mass density reported by the manufacturers and measured compressional velocities).

### Characterizing Flip-Chip Underfill Process Variations

Acoustic images (Figures 2 and 3) of the die/underfill interface show regions with distinctly different amplitudes of reflection. These changes in reflected amplitude are a result of changes in the acoustic impedance mismatch. This principle is used to calculate the impedance of the flaw ( $Z_{Flaw}$ ) relative to the impedance of the normal background ( $Z_{Underfill}$ ).

Ultrasonic pulses are reflected at any interface when there is a change in the acoustic impedance from one medium (material 1) to the next (material 2). At normal ( $90^\circ$ ) incidence, the reflected amplitude is related to the incident amplitude by the relationship

$$A_{Reflected} = R_{12} A_{Incident} \quad (4)$$

where  $R_{12}$  is the reflection coefficient for sound incident from material 1 onto material 2, given by

$$R_{12} = \frac{Z_2 - Z_1}{Z_2 + Z_1} \quad (5)$$

For a pulse incident from Silicon onto the underfill (normal region), the reflection coefficient is given by

$$R_{Si-Underfill} = \frac{Z_{Si} - Z_{Underfill}}{Z_{Si} + Z_{Underfill}} \quad (6)$$

To determine ( $R_{Si-Underfill}$ ), the impedance of silicon and the normal underfill must be known. Silicon is anisotropic and the values of the velocity vary with direction of propagation and polarization. Lacking information about the precise crystallographic orientation of the Si die, the wafers are assumed to possess a {100} orientation, with compressional waves propagating in the [100] direction (polarization also in  $\langle 100 \rangle$  direction). From velocity and density values reported in literature (Dieulesaint and Royer, 1980), the impedance of silicon in the  $\langle 100 \rangle$  direction is calculated to be 19.7 MRayl. Alternatively, a value of 21.9 MRayl could have been used (assuming a wafer orientation of {111}). Assuming a {100} orientation for the Si die is not expected to affect the validity of the conclusions since relative changes in the underfill properties are the focus in this study. However, the error in the predicted absolute values of impedance is expected to be only 5% (approximately) even if the correct orientation is {111} instead of {100}. The impedance of the underfill is not known and will be determined based on a model of the elastic properties.

The A-scans from the flawed regions ( $A_{Flaw}$ ) and normal underfill regions ( $A_{Underfill}$ ) as seen from the acoustic images, are used to compute the ratio:

$$\beta = \frac{A_{Underfill}}{A_{Flaw}} \quad (7)$$

The impedance of the flawed region is determined from a known (or assumed) reflection coefficient in the normal underfill region using the equation:

$$Z_{Flaw} = Z_{Si} \left( \frac{\beta + R_{Si-Underfill}}{\beta - R_{Si-Underfill}} \right) \quad (8)$$

Micromechanical modeling is used to determine the elastic properties based on the acoustic impedance determined (using equation 8).

### Modeling Elastic Properties of a Composite

Modern plastic encapsulants used in IC packaging are largely composed of fused silica filler (>50% by weight), epoxy resin and hardener. The filler typically consists of a combination of *spherical* and *ground* fused silica in a broad size distribution (Pecht et al., 1995). Although other additives are present for stress reduction, fire retardation, etc., it is assumed that the elastic properties are dominated by the polymer matrix and the volume fraction of the filler. In other words, the encapsulant is treated as a two-phase composite: a polymer matrix reinforced with silica particles.

Various models have been put forth to predict the elastic properties of dual phase composites. The lower and upper bounds predicted by the Hashin-Shtrikman model provide the most restrictive estimates on the bulk moduli if only constituent properties and volume fraction are known (Watt et al., 1976). The bounds of Hashin and Shtrikman (1963) are based on variational principles, and do not involve any assumption of the shape of the reinforcement (filler) or the matrix (epoxy). Boucher (1974) has shown that the self-consistent solution approximation model for disk shaped reinforcement corresponds to these bounds. A stiffer phase as the reinforcement in a softer matrix yields the HS<sup>-</sup> bound while the case of a stiffer matrix yields the HS<sup>+</sup> bound (Watt et al., 1976).

In this study, it is hypothesized that the HS<sup>-</sup> bound describes the elastic behavior of the polymer composite, namely the soft epoxy reinforced with stiffer silica particles. This hypothesis is validated using two sets of samples:

- 1) Controlled calibration specimens made with a known resin reinforced with glass spheres of known properties, size and volume fraction
- 2) Real specimens of commercial molding compounds for which the constituent properties, volume fraction and composition are known approximately.

Predictions of the compressional and shear ultrasonic velocities are made using the known properties of the matrix and filler using the HS<sup>-</sup> model. These are then compared to measured ultrasonic velocities. The velocities of the calibration specimens were predicted using the properties of soda lime glass ( $\rho = 2250 \text{ kg/m}^3$ ) and clear epoxy resin ( $\rho = 1125 \text{ kg/m}^3$ ) with compressional and shear wave velocities of, respectively, 2545 and 1110 m/s, and 6000 and 3765 m/s.

For the controlled system, clear polyester casting resin was reinforced with various volume fractions of nominally 100 and 200  $\mu\text{m}$  soda lime glass particles. The glass particles were shaped roughly in the form of spheroids and ranged in size from 85 to 120  $\mu\text{m}$  and 170 to 230  $\mu\text{m}$  for the two nominal sizes, respectively. The nominal fraction of the beads ranged from 0 % (neat resin) to 10 % by volume in the specimen set. The

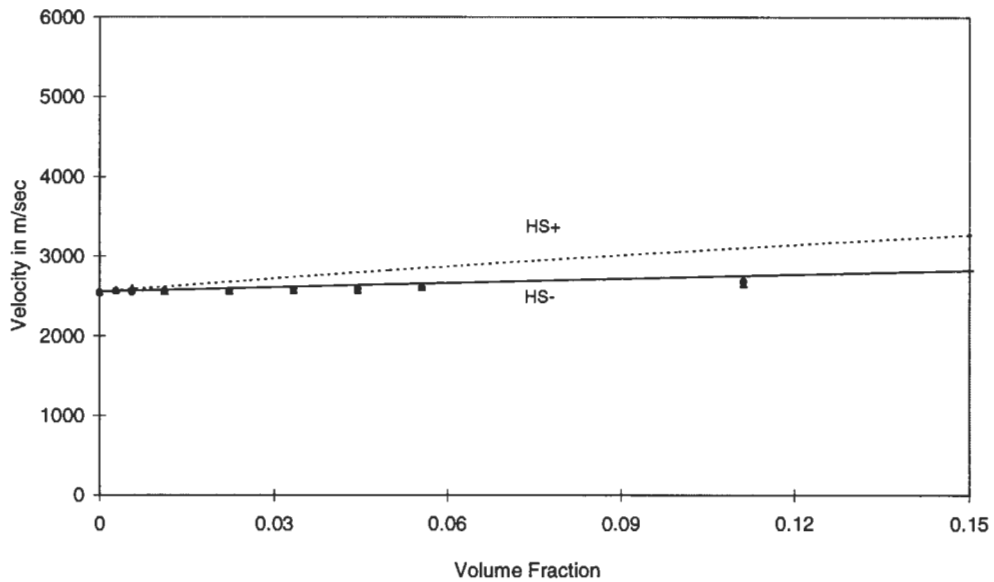


**Figure 4. Comparison of the measured compressional wave velocities of calibration specimens with the predictions from the Hashin-Shtrikman model.**

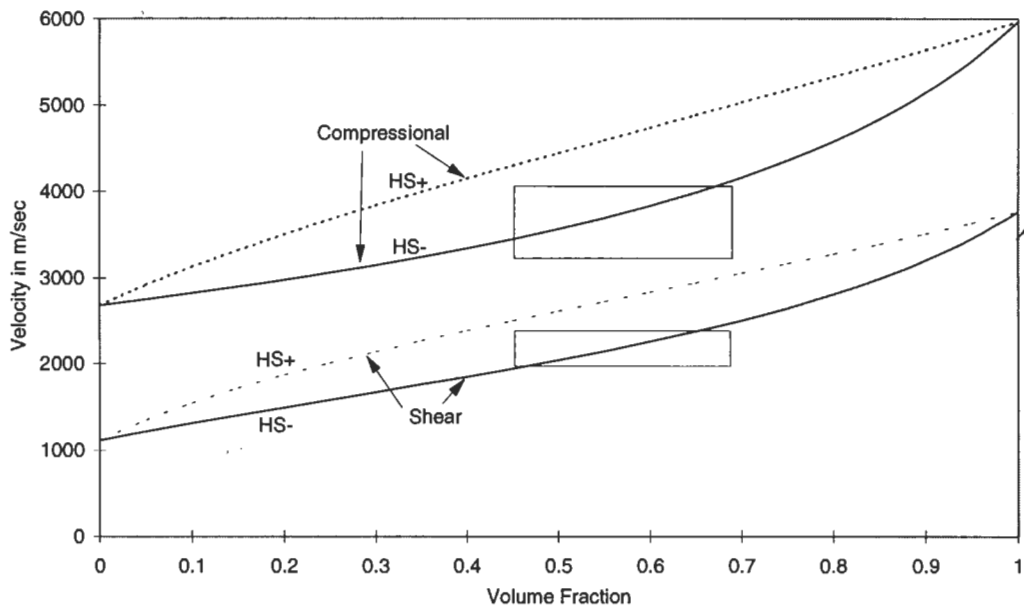


**Figure 5. Compressional and shear wave velocity of molding compounds compared to the predictions of the Hashin-Shtrikman bounds.**

comparison of the model predictions and the measured velocities are shown in Figure 4.

For the real systems, commercial epoxy molding compounds were used. The properties of fused silica and epoxy<sup>1</sup> (Selfridge,

<sup>1</sup> DER 332, cured with 15% by weight of hardener, Dow Chemical and E.T.Horn Co. (Oakland, CA)

**Table 1. Samples for which engineering moduli were determined.**

Compound <sup>2</sup>	Filler Loading (weight %)	Low stress additives	Resin type	Density (kg/m <sup>3</sup> )	Thickness (mm)
MP8000CH	Medium-high	Medium	OCN	1940	3.22
MP190ML	Medium	High	OCN	1860	3.20
6300HA	Low (~60%)	High	OCN	1820	3.20
7320CR	High (~80%)	Low	Biphenyl	1920	3.21

**Table 2. Measured Time of flight (TOF) data, and calculated ultrasonic velocity and impedance data for the molding compound samples.**

Compound	Compressional TOF (µsec)	Compressional Velocity (m/sec)	Shear TOF (µsec)	Shear Velocity (m/sec)	Calculated Z (MRayl)
MP8000CH	1.580	4070	2.689	2392	7.9
MP190ML	1.838	3480	3.271	1955	6.4
6300HA	1.965	3260	3.455	1854	5.9
7320CR	1.652	3881	2.947	2175	7.5

1985) were used in modeling the compressional and shear velocities. The comparison between the predicted and measured velocities for molding compounds is shown in Figure 5 for the compressional and shear cases. The precise volume fraction of filler in the molding compounds could not be found in open literature. Therefore, the measured velocities are shown by a rectangle whose height represents the range of measured velocity values and whose width represents the approximate range of volume fractions from the material data sheets.

As can be seen in the figures, the known and real systems agree well with the use of the HS<sup>+</sup> bound, thus validating its use.

In this study, acoustic impedance is used to gauge the elastic properties of the underfill. Results of the modeling showed that the acoustic impedance was sensitive to the volume fraction of the filler (Figure 6) suggesting its appropriateness as an indicator of the elastic properties. Table 5 presents the engineering properties predicted by the HS<sup>+</sup> bound for volume fraction of filler ranging from 0 to 1. The values of the matrix and reinforcement used in modeling the polymer composites are represented by the 0 and 1 volume fraction, respectively.

## EXPERIMENT

Two experimental schemes are required in this study: time of flight data to determine the engineering moduli of molding compounds and echo amplitude data to characterize the process variations in the flip-chip underfill.

### Time of Flight

The samples used to determine the engineering moduli of molding compounds were flat, tensile test coupons of uniform

<sup>2</sup> MP8000CH and MP190ML are manufactured by Nitto Denko America (Fremont, CA), and 6300HA and 7320CR by Sumitomo Plastics America, Inc. (Santa Clara, CA).

thickness. The coupons were molded using the standard parameters recommended by the manufacturers for mold temperature, time and pressure and for post-mold cure time and temperature. Relevant properties from the manufacturers' data sheets are presented in Table 1.

The equipment used to measure the time of flight included an acoustic microscope (C-SAM<sup>3</sup>), a leveling fixture, and two transducers<sup>4</sup>. An unfocused, immersion transducer (Model #A309S, 5 MHz, 12.57 mm element diameter) was used for generating compressional waves. An unfocused, shear wave, contact transducer (Model #V156, 5 MHz 6.125 mm element diameter) was used for generating shear waves. Water was used as the coupling medium for the immersion transducer; and a thin layer of maple syrup was used as the couplant for the shear wave contact transducer.

A standard time of flight procedure for measuring ultrasonic velocity was used: a) the ultrasonic pulse is generated electronically b) the return signal (the A-scan) is displayed on an oscilloscope and digitized, and c) the time difference between corresponding peaks of the front surface echo and the back surface echo are measured for the compressional ( $\Delta t_c$ ) and shear modes ( $\Delta t_s$ ).

### Echo Amplitude

The samples used to characterize underfill processing variations consisted of the following commercial flip-chip packages a) two samples of die size 4.9 mm x 3.9 mm b) three samples of die size 6.75 x 6.75 mm.

The equipment used to measure the echo amplitude included an acoustic microscope (C-SAM) and a focused, delay-line,

<sup>3</sup> C-SAM is manufactured by Sonoscan, Inc (Bensenville, IL).

<sup>4</sup> All transducers used here were made by Panametrics, Inc. (Waltham, MA)

**Table 3. Calculated Impedance and Engineering moduli of the molding compound samples.**

Compound	$\nu$	$\mu$ (GPa)	$\kappa$ (GPa)	E (GPa)
MP8000CH	0.236	11.10	17.34	27.44
MP190ML	0.269	7.11	13.05	18.05
6300HA	0.261	6.26	11.00	15.78
7320CR	0.271	9.31	16.79	23.09

immersion transducer (Model #V3194, 100 MHz, 6.125 mm element diameter, 12.7 mm focal length). Water was used as the coupling medium. The procedure consisted of:

1. Immersing the sample in the water bath
2. Centering the scanner over the die and leveling the stage
3. Focusing on the die/underfill interface by changing the distance between the transducer and the sample until the compressional wave echo from this interface was maximized
4. Acquiring a full gray-scale image of the entire die area
5. Measuring the peak-to-peak amplitude of the die/underfill interface echo, via the A-scan display, at multiple locations that were chosen based on the image acquired in step 4.

## RESULTS AND DISCUSSION

### Engineering Moduli of Molding Compounds

Table 2 presents the time of flight data, and the calculated ultrasonic velocities and the acoustic impedances. The engineering moduli are presented in Table 3.

The published values of density from the data sheets are used in calculating the moduli. Instead, density values could have been determined from the measured acoustic impedances using equation 3. This was not done in this study because a minor discrepancy was observed between values obtained by the measured and theoretically calculated acoustic impedances. The compressional acoustic impedance values presented here are, on the average, 10% higher than the values measured ultrasonically by Canumalla and Kessler (1997). The differences are not due to systematic errors in the technique because measurements on smooth specimens of homogeneous Lucite did not exhibit any discrepancy between the theoretical and measured acoustic impedances. A better understanding of possible sources of error will enable a quick and nondestructive determination of the density from ultrasonic measurements of acoustic impedance. Then, the engineering moduli of molding compounds can be determined solely from ultrasonic measurements without requiring a separate measurement of mass density.

### Characterizing Flip-Chip Underfill Process Variations

The images of two different kinds of flip chip packages are shown in Figure 2 and 3. In both cases, the image of the die-underfill interface shows variations due to non-optimal flow of the underfill.

In Figure 2, areas having three different reflectivities can be seen in the underfilled region: I) normal background area II) lighter gray areas and III) bright white areas. The amplitudes of the reflected echoes at this interface were measured over different

areas in two chips and the averages for each chip are shown in Table 4. Assuming a typical filler volume fraction in the base material of about 40% (approximately 55-60% by weight, Suryanarayana, 1991), the HS<sup>-</sup> model (see Table 5) predicts an acoustic impedance of approximately 5.5 MRayl. Using this value for region I, the acoustic impedance for areas II and III are

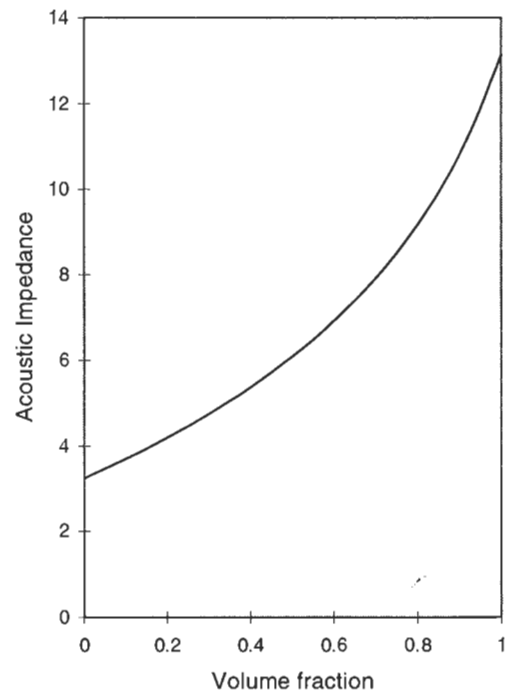


**Figure 6. Effect of fused silica filler on the acoustic impedance as predicted by the HS<sup>-</sup> bound.**

calculated to be approximately 3 (close to that of the unfilled resin) and 0, respectively. Thus, the light gray areas appear to be composed primarily of resin while the bright areas are voids or are delaminated. Since both lower filler content and disbonds increase the reflection coefficient without changing the polarity of the echo, the ability to measure a zero impedance makes it possible to unambiguously differentiate between them.

It is also possible to extract quantitative information about the filler content from the calculated acoustic impedance and the predictions of the model. In Figure 3, "fingers" of lighter shade (II) are visible against the background (I). It is generally believed that these inhomogeneities are caused by filler segregation during flow of the underfill. Assuming that the well bonded material has an impedance of about 5.5 MRayl, the material in the fingers is

**Table 4. Measured amplitudes at the die/underfill interface at the different regions**

	Sample ID	Area (I)	Area (II)	Area (III)	Z <sub>i</sub>	Z <sub>ii</sub>	Z <sub>iii</sub>
Fig. 2	A	32.50	42.20	57.74	5.5	3.05	-0.01
	B	33.03	43.37	57.22	5.5	2.94	0.24
	C	41.67	48.65	-	5.5	4.06	-
Fig. 3	D	41.53	48.78	-	5.5	4.01	-
	E	41.61	50.07	-	5.5	3.78	-

estimated to have an impedance of approximately 3.9 MRayl. From Table 5, the filler content is estimated to be about 0.15 (or 26% lower). The Young's modulus can be predicted to be 7 GPa (approximately 50% lower than the base value of 14 GPa) and the CTE is predicted to be  $41 \times 10^{-6} / ^\circ\text{C}$  (approximately 57% higher than the base value of  $26 \times 10^{-6} / ^\circ\text{C}$ ).

A recent analytical study (Michaeledes and Sitaraman, 1997) found that a 20% reduction in the stiffness of the underfill could degrade the fatigue of a flip chip device life by about 11%. It was, therefore, deemed to be a relatively less severe flaw compared to voiding. However, if filler settling causes a 50% degradation in the stiffness, with a 50% increase in CTE, as found in the present study, these flaws could prove more detrimental than previously believed. Further work involving acoustic microscopy in conjunction with thermal cycling will be needed to better assess the reliability impact of such flaws.

## CONCLUSIONS

The procedures and rationale for measuring the elastic properties of polymer based materials nondestructively are discussed in this study. The acoustic microscope is exploited for quantitative, *in situ* material property measurement in electronic packages over a microscopic area.

The engineering moduli (shear, bulk and Young's moduli and the Poisson's ratio) of 4 molding compounds (7320CR, 6300HA, MP 190ML and MP 8000CH) were determined using this approach, nondestructively. There was considerable variation in the Young's (15 to 27 GPa), shear (6 to 11 GPa) and bulk moduli (11 to 17 GPa). The size of the filler has little influence on the ultrasonic properties indicating that the same model may be applicable even if the filler size is different.

In flip chip packages, processing related material property variations in the underfill were characterized by acoustic microscopy. The Hashin-Shtrikman lower (HS<sup>-</sup>) bound is appropriate for this class of materials and showed good correlation to measured ultrasonic velocities both in calibration specimens and commercial molding compounds. Areas of lower filler content were distinguishable from disbonded areas even though polarity of the reflected echo is same for both cases. Not only could a disbond be distinguished from a resin rich area, the volume fraction of filler and elastic properties were also quantified. For example, resin rich areas are predicted to have a filler volume fraction of 0.15 as compared to 0.40 for the base material. This filler content would result in a Young's modulus and CTE of 7 GPa and  $41 \times 10^{-6} / ^\circ\text{C}$ , as compared to a base value of 14 GPa and  $26 \times 10^{-6} / ^\circ\text{C}$ , respectively. Techniques presented in this paper are believed to be attractive for advanced process

control, rapid yield management and for providing input into package reliability studies (such as finite element analysis).

## ACKNOWLEDGEMENTS

This work was funded by the IR&D Program of Sonoscan, Inc.

## REFERENCES

- Boucher, S., 1974, "On the Effective Moduli of Isotropic Two-phase Elastic Composites," *Journal of Composite Materials*, **8**, pp. 82-89.
- Canumalla, S. and Kessler, L. W., 1997, "Towards a Nondestructive Procedure for Characterization of Molding Compounds," *35<sup>th</sup> International Reliability Physics Symposium*, pp. 149-155.
- Canumalla, S., Gordon, G. A., and Pangborn, R. N., 1997, "In situ measurement of the Young's Modulus of an Embedded Inclusion by Acoustic Microscopy," *Journal of Engineering Materials and Technology*, **119** (2), pp. 143-147.
- Dieulesaint, E. and Royer, D., 1980, "Elastic Waves in Solids," John Wiley and Sons, New York.
- Hashin, Z., and Shtrikman, S., 1963, "A Variational Approach to the Elastic Behavior of Multiphase Materials," *Journal of the Mechanics and Physics of Solids*, **11**, pp. 127-140.
- Krautkramer, J., and Krautkramer, H., 1983, "Ultrasonic Testing of Materials," Springer-Verlag, New York.
- Michaelides, S., and Sitaraman, S., 1997, "Role of Underfilling Imperfections on Flip-chip Reliability," *Advances in Electronic Packaging*, **EPP-19** (2), pp. 1487-1493.
- Pecht, M. G., Nguyen, L. T., and Hakim, E. B., 1995, "Plastic Encapsulated Microelectronics," John Wiley and Sons, New York.
- Selfridge, A. R., 1985, "Approximate Materials in Isotropic Materials," *IEEE Transactions on Sonics and Ultrasonics*, **SU-32** (3), pp. 382-394.
- Suryanarayana, D., Hsiao, R., Gall, T. P., and McCreary, J.M., 1991, "Enhancement of Flip-chip Fatigue Life by Encapsulation," *IEEE Transactions on Components, Hybrids, and Manufacturing Technology*, **14** (1), pp. 218-223.
- Taylor, S. A., Chen, K., and Mahajan, R., 1997, "Moisture Migration and Cracking in Plastic Quad Flat Packages," *Journal of Electronic Packaging*, **119** (2), pp. 85-88.
- Watt, P. J., Davies, G. F., and O'Connell, R. J., 1976, "The Elastic Properties of Composite Materials," *Reviews of Geophysics and Space Physics*, **14** (4), pp. 541-563.

**Table 5. Predictions of the Hashin-Shtrikman lower bound. Properties of constituents are shown as values for 0 and 1 volume fraction.**

Weight Fraction	Volume Fraction	$\rho$ (kg/m <sup>3</sup> )	$\kappa$ (GPa)	$\mu$ (GPa)	E (GPa)	$\nu$	$V_{Compressional}$ (m/s)	$V_{Shear}$ (m/s)	$Z_{Compressional}$ (MRayl)	CTE (10 <sup>-6</sup> /°C)
0	0	1210.0	6.70	1.49	4.16	0.40	2680	1110.0	3.24	50
0.09	0.05	1259.5	7.05	1.85	5.10	0.38	2749	1211.8	3.46	46.99
0.17	0.1	1309.0	7.43	2.24	6.10	0.36	2821	1307.6	3.69	44.05
0.24	0.15	1358.5	7.85	2.66	7.17	0.35	2896	1399.4	3.93	41.18
0.31	0.2	1408.0	8.30	3.12	8.32	0.33	2975	1488.9	4.19	38.37
0.38	0.25	1457.5	8.80	3.63	9.56	0.32	3058	1577.2	4.46	35.62
0.44	0.3	1507.0	9.34	4.18	10.91	0.31	3146	1665.5	4.74	32.93
0.49	0.35	1556.5	9.94	4.79	12.39	0.29	3240	1754.8	5.04	30.30
0.55	0.4	1606.0	10.62	5.47	14.01	0.28	3340	1846.2	5.36	27.72
0.60	0.45	1655.5	11.37	6.23	15.81	0.27	3448	1940.6	5.71	25.20
0.65	0.5	1705.0	12.21	7.09	17.82	0.26	3565	2039.2	6.08	22.73
0.69	0.55	1754.5	13.18	8.06	20.08	0.25	3692	2143.2	6.48	20.31
0.73	0.6	1804.0	14.28	9.17	22.65	0.24	3833	2254.1	6.91	17.94
0.77	0.65	1853.5	15.55	10.44	25.60	0.23	3988	2373.6	7.39	15.61
0.81	0.7	1903.0	17.04	11.93	29.02	0.22	4161	2503.9	7.92	13.33
0.85	0.75	1952.5	18.81	13.69	33.05	0.21	4357	2647.7	8.51	11.10
0.88	0.8	2002.0	20.94	15.80	37.86	0.20	4580	2808.9	9.17	8.91
0.91	0.85	2051.5	23.55	18.37	43.73	0.19	4839	2992.2	9.93	6.76
0.94	0.9	2101.0	26.84	21.58	51.05	0.18	5145	3204.8	10.81	4.66
0.97	0.95	2150.5	31.10	25.70	60.45	0.18	5513	3457.1	11.86	2.59
1	1	2200.0	36.83	31.19	72.96	0.17	5970	3765.0	13.13	0.56